American Journal of Pathology, Vol. 165, No. 4, October 2004

Stem Cells, Tissue Engineering and Hematopoietic Elements

Deficient Eosinophil Chemotaxis-Promoting Activity of Genetically Normal Mast Cells Transplanted into Subcutaneous Tissue of *Mitf*$^{mi\text{-}vga9}$/*Mitf*$^{mi\text{-}vga9}$ Mice

Comparison of the Activity and Mast Cell Distribution Pattern with Kit^{W}/Kit$^{W\text{-}v}$ *Mice*

Keisuke Oboki, Eiichi Morii, and Yukihiko Kitamura

From the Department of Pathology, Graduate School of Frontier Bioscience and Medical School, Osaka University, Osaka, Japan

Despite the practical lack of mast cells in the skin tissue of WBB6F$_1$-Kit^{W}/*Kit*$^{W\text{-}v}$, the skin tissue of WBB6F$_1$-*Mitf*$^{mi\text{-}vga9}$/*Mitf*$^{mi\text{-}vga9}$ mice contains one third of mast cells than that of WBB6F$_1$-+/+ mice. We attempted to investigate the function of the decreased but appreciable number of mast cells in the skin of WBB6F$_1$-*Mitf*$^{mi\text{-}vga9}$/*Mitf*$^{mi\text{-}vga9}$ mice. The substance P (SP)-induced eosinophil infiltration was examined using air-bleb assay. The air-bleb membrane was composed of the subcutaneous connective tissue. Unexpectedly, we found that the air-bleb membranes formed in the back of WBB6F$_1$-*Mitf*$^{mi\text{-}vga9}$/*Mitf*$^{mi\text{-}vga9}$ mice contained no mast cells. The WBB6F$_1$-*Mitf*$^{mi\text{-}vga9}$/*Mitf*$^{mi\text{-}vga9}$ mice showed impaired SP-induced eosinophil infiltration as observed in WBB6F$_1$-*Kit*^{W}/*Kit*$^{W\text{-}v}$ mice, indicating that mast cells detected in the dermis of WBB6F$_1$-*Mitf*$^{mi\text{-}vga9}$/*Mitf*$^{mi\text{-}vga9}$ mice did not help SP-induced eosinophil infiltration. Subcutaneous transplantation of cultured mast cells from WBB6F$_1$-+/+ mice normalized SP-induced eosinophil infiltration in WBB6F$_1$-*Kit*^{W}/*Kit*$^{W\text{-}v}$ mice but not in WBB6F$_1$-*Mitf*$^{mi\text{-}vga9}$/*Mitf*$^{mi\text{-}vga9}$ mice. The greater number and the more dispersed distribution pattern of mast cells that appeared in the subcutaneous connective tissue of WBB6F$_1$-*Kit*^{W}/*Kit*$^{W\text{-}v}$ mice after the transplantation appeared to explain the difference between WBB6F$_1$-*Kit*^{W}/*Kit*$^{W\text{-}v}$ and WBB6F$_1$-*Mitf*$^{mi\text{-}vga9}$/*Mitf*$^{mi\text{-}vga9}$ mice. *(Am J Pathol 2004, 165:1141–1150)*

Three mast cell-deficient mutants have been reported; ie, mice of *Kit*^{W}/*Kit*$^{W\text{-}v}$,[1] *Kitl*^{Sl}/*Kitl*$^{Sl\text{-}d}$,[2] and *Mitf*$^{mi\text{-}vga9}$/*Mitf*$^{mi\text{-}vga9}$ genotypes.[3,4] *Kit*^{W}/*Kit*$^{W\text{-}v}$ mice have two mutant alleles at the *W* locus that encode c-*kit* receptor tyrosine kinase (KIT).[5,6] *Kitl*^{Sl}/*Kitl*$^{Sl\text{-}d}$ mice have two mutant alleles at the *Sl* locus that encode KIT ligand (KITL).[7–10] KITL-KIT signals are essential for development and survival of mast cells. Tissues of adult *Kit*^{W}/*Kit*$^{W\text{-}v}$ and *Kitl*^{Sl}/*Kitl*$^{Sl\text{-}d}$ mice contain <1% mast cells than that of control wild-type (+/+) mice.[1,2] *Mitf*$^{mi\text{-}vga9}$/*Mitf*$^{mi\text{-}vga9}$ mice do not express microphthalmia-associated transcription factor (MITF) because of the insertion of a transgene at the promoter region of *Mitf* gene.[11] Despite the practical lack of mast cells in the skin tissue of *Kit*^{W}/*Kit*$^{W\text{-}v}$ and *Kitl*^{Sl}/*Kitl*$^{Sl\text{-}d}$ mice, the skin tissue of *Mitf*$^{mi\text{-}vga9}$/*Mitf*$^{mi\text{-}vga9}$ mice contains one third of mast cells than that of control +/+ mice.[12–16] Moreover, skin mast cells of *Mitf*$^{mi\text{-}vga9}$/*Mitf*$^{mi\text{-}vga9}$ mice appear to have connective tissue-type phenotype because they were stained with berberine sulfate, suggesting the content of heparin.[17] No mast cells are detected in tissues other than the skin of *Mitf*$^{mi\text{-}vga9}$/*Mitf*$^{mi\text{-}vga9}$ mice, such as the lung, spleen, stomach, and peritoneal cavity.[18]

Functions of skin mast cells have been investigated using (WB × C57BL/6)F$_1$ (WBB6F$_1$)-*Kit*^{W}/*Kit*$^{W\text{-}v}$ mice.[19] Intact WBB6F$_1$-*Kit*^{W}/*Kit*$^{W\text{-}v}$ mice were compared with rescued WBB6F$_1$-*Kit*^{W}/*Kit*$^{W\text{-}v}$ mice that had received the transplantation of cultured mast cells (CMCs) derived from WBB6F$_1$-+/+ mice. Wershil and colleagues[20] demonstrated that mast cells were essential for IgE-dependent immediate hypersensitivity reaction. The IgE-dependent extravasation of fibrinogen did not occur in the skin

Supported by a Grant-in-Aid for Specially Promoted Research from the Ministry of Education, Culture, Sports, Science, and Technology, Japan.

Accepted for publication June 10, 2004.

Address reprint requests to Eiichi Morii, Department of Pathology (Room C2), Graduate School of Frontier Bioscience and Medical School, Osaka University, 2-2 Yamada-oka, Suita, Osaka, 565-0871, Japan. E-mail: morii@patho.med.osaka-u.ac.jp.

of intact WBB6F$_1$-*Kit^W/Kit$^{W\text{-}v}$* mice but did occur in the skin of WBB6F$_1$-*Kit^W/Kit$^{W\text{-}v}$* mice whose mast cell depletion was rescued by the prior subcutaneous injection of WBB6F$_1$-+/+ CMCs. In contrast to the case of the IgE-dependent immediate hypersensitivity reaction, the presence of mast cells was not essential for neutrophil infiltration induced by phorbol 12-myristate 13-acetate.[21] However, the presence of mast cells augmented the neutrophil infiltration. Cutaneous eosinophil infiltration induced by substance P (SP) was examined by Matsuda and colleagues.[22] They showed that SP-induced eosinophil infiltration was dependent on the presence of mast cells using air-bleb assay. Yano and colleagues[23] injected SP into the ear skin of mice and found the requirement of mast cells for augmentation of SP-induced granulocyte infiltration. In these experiments, a granulocyte infiltration of low level was observed in the skin of intact WBB6F$_1$-*Kit^W/Kit$^{W\text{-}v}$* mice, but the prior injection of +/+ CMCs significantly augmented the infiltration.

Because the skin of WBB6F$_1$-*Mitf$^{mi\text{-}vga9}$/Mitf$^{mi\text{-}vga9}$* mice contains one third of mast cells than that of WBB6F$_1$-+/+ mice, we attempted to investigate the function of the decreased but appreciable number of mast cells in the skin of WBB6F$_1$-*Mitf$^{mi\text{-}vga9}$/Mitf$^{mi\text{-}vga9}$* mice. The SP-induced eosinophil infiltration was examined in the skin tissue of intact WBB6F$_1$-*Mitf$^{mi\text{-}vga9}$/Mitf$^{mi\text{-}vga9}$* mice using air-bleb assay. Unexpectedly, we found that the air-bleb membranes formed in the back of WBB6F$_1$-*Mitf$^{mi\text{-}vga9}$/Mitf$^{mi\text{-}vga9}$* mice contained no mast cells. Histological study revealed that the air-bleb membrane was composed of the subcutaneous connective tissue. Mast cells were present in the dermis but not in the subcutaneous connective tissue of WBB6F$_1$-*Mitf$^{mi\text{-}vga9}$/Mitf$^{mi\text{-}vga9}$* mice. The intact WBB6F$_1$-*Mitf$^{mi\text{-}vga9}$/Mitf$^{mi\text{-}vga9}$* mice showed impaired SP-induced eosinophil infiltration. Moreover, the prior injection of WBB6F$_1$-+/+ CMCs into the subcutaneous connective tissue of WBB6F$_1$-*Mitf$^{mi\text{-}vga9}$/Mitf$^{mi\text{-}vga9}$* mice did not increase the level of the SP-induced eosinophil infiltration. The different number and distribution pattern of subcutaneously injected WBB6F$_1$-+/+ CMCs between WBB6F$_1$-*Kit^W/Kit$^{W\text{-}v}$* and WBB6F$_1$-*Mitf$^{mi\text{-}vga9}$/Mitf$^{mi\text{-}vga9}$* mice appeared to explain the result.

Materials and Methods

Mice

Details of WBB6F$_1$-*Mitf$^{mi\text{-}vga9}$/Mitf$^{mi\text{-}vga9}$* mice, previously called WBB6F$_1$-*tg/tg* mice, were described elsewhere.[18] According to standard nomenclature of mutant alleles provided by Mouse Genome Informatics (*www.informatics.jax.org*), we changed the designation from *tg* to *Mitf$^{mi\text{-}vga9}$*. WBB6F$_1$-*Mitf$^{mi\text{-}vga9}$/Mitf$^{mi\text{-}vga9}$* mice were bred in our laboratory. WBB6F$_1$-*Kit^W/Kit$^{W\text{-}v}$* and WBB6F$_1$-+/+ mice were purchased from the Japan SLC (Hamamatsu, Japan). All mice were used at 2 to 5 months of age unless stated otherwise and were kept under specific pathogen-free conditions in our animal facility.

Air-Bleb Assay

Infiltration of eosinophils into the mouse skin tissue was estimated by air-bleb assay as described by Lawman and colleagues.[24] Briefly, under anesthesia with 50 mg/kg of Nenbutal (Dainippon Pharmaceutical, Osaka, Japan), a volume of 0.9 ml of air was slowly injected into the shaved dorsal skin via a 27-gauge needle with a 1-ml syringe to form an air-bleb, and then 0.1 ml of saline (Otsuka Pharmaceutical, Tokyo, Japan) containing 10^{-5} mol/L SP (Sigma-Aldrich, St. Louis, MO), saline containing 300 ng/ml of leukotriene B$_4$ (LTB$_4$) (Sigma-Aldrich), or saline alone, which was present in the same syringe was immediately introduced into the air-bleb. Four hours after the injection, the mice were killed by overinhalation of ether. An interval of 4 hours was chosen according to the result of Matsuda and colleagues.[22] The thin connective tissue membrane surrounding the air-bleb was carefully removed and gently stretched onto a glass slide. After air-drying, the specimens were fixed with methanol at room temperature for 10 minutes. They were transferred to a staining jar containing Giemsa's solution (Merck, Darmstadt, Germany) freshly 1:10 diluted with phosphate buffer (pH 6.4) (Merck), and were stained for 10 minutes. After washing with water and air-drying, they were cleared with xylene for three times and were mounted with Permount (Fisher Scientific, Pittsburgh, PA). Ten fields were examined per specimen at a magnification of ×400. Fields that gave high contrast between eosin-positive cells and other cells were selected at random. The number of eosinophils shown in the result represented the total of eosinophils counted in 10 fields. Air-blebs were sampled at 4, 12, and 24 hours after SP injection. The number of infiltrating eosinophils at particular times after administration of SP was divided by the mean number of eosinophils at the same time after administration of saline alone, and the calculated ratio was used as an index for eosinophil infiltration at indicated time points.

Number and Distribution Pattern of Mast Cells

To count mast cells in the dermis, the dorsal skin was removed and smoothed onto a piece of filter paper to keep them flat, fixed in Carnoy's fluid (60% methanol, 30% chloroform, 10% acetic acid), and embedded in paraffin. Sections (4 μm thick) of skin pieces were stained with Alcian blue. Mast cells were counted at a magnification of ×200. The number was expressed as mast cells per square millimeter of dermis.

To count mast cells in the subcutaneous connective tissue, a volume of 1-ml of air was injected into the shaved dorsal skin and air-bleb membranes were prepared as describe above. These air-bleb membranes were stained by Giemsa's solution. Mast cells were counted as described above in the case of the dermis.

To estimate distribution pattern of injected CMCs in air-bleb membranes, two methods were used. First, we counted 10 fields per Giemsa-stained specimen as described above, and a proportion of fields containing ≥10

mast cells was determined. Second, we stained the air-bleb membranes with a fluorescence dye, berberine sulfate (Sigma-Aldrich), to highlight only mast cells.[17] The specimens were examined by PROVIS AX80 microscope (Olympus, Tokyo, Japan). With this staining, the distribution pattern of mast cells was recognized more easily than with Giemsa staining.

Cellular Area and Fluorescent Intensity

Specimens stained with berberine sulfate were examined with a LSM510 confocal microscope (Carl Zeiss, Oberkochen, Germany). Fluorescent images were collected and processed by a Macintosh computer (Apple Computer, Cupertino, CA). Color information was removed from microscopic images using Adobe Photoshop 7.0 software. Fluorescent cellular region was measured using the public domain NIH Image program (developed at the National Institutes of Health and available on the internet at *http://rsb.info.nih.gov/nih-image/*). Briefly, the scale was set by using a scale bar in the image. Each fluorescent cell shape was surrounded by using a free line tool. After area and integrated density were selected in the measurement option, the values of the measurement were obtained. The values of integrated density were used for the values of intensity.

Transplantation of CMCs

Pokeweed mitogen-stimulated spleen cell-conditioned medium was prepared according to the method described by Nakahata and colleagues.[25] Spleen cells of WBB6F$_1$-+/+ mice were cultured in α-MEM (ICN Biomedicals, Aurora, OH) supplemented with 20% pokeweed mitogen-stimulated spleen cell-conditioned medium and 10% fetal calf serum (Nippon Bio-Supp Center, Tokyo, Japan) for 4 to 5 weeks.[12,18]

CMCs were harvested, washed, and resuspended in α-MEM at a concentration of 1.0×10^6 cells/0.2 ml. Seven subcutaneous injections were done in the shaved dorsal skin of WBB6F$_1$-*Kit*^{W}/*Kit*$^{W\text{-}v}$ and WBB6F$_1$-*Mitf*$^{mi\text{-}vga9}$/*Mitf*$^{mi\text{-}vga9}$ mice. Control mice were injected with culture medium alone. Six weeks after the injection, the air-bleb was produced at the injection site of CMCs.

Number of Eosinophils in Peripheral Blood

Eosinophils were counted on smears of peripheral blood. The smears were air-dried and fixed in methanol for 10 minutes. They were transferred to a staining jar containing Hansel's solution freshly diluted with an equal volume of phosphate buffer (pH 7.2, Merck), and stained for 5 minutes. A content of Hansel's solution was 1% methylene blue and 0.33% eosin Y in methanol. Two hundred nucleated cells were counted at a magnification of ×400.

Bone Marrow Transplantation

A Radioflex 350 X-ray machine (Rigaku, Tokyo, Japan) operated at 180 kV and 15 mA with 1-mm aluminum filter (0.885 Gy/min) was used. Mice were kept in a polypropylene box during irradiation. Bone marrow cells were prepared as described previously.[26] Bone marrow cells (1.0×10^7) of WBB6F$_1$-+/+ mice were injected intravenously to eight Gy-irradiated WBB6F$_1$-*Mitf*$^{mi\text{-}vga9}$/*Mitf*$^{mi\text{-}vga9}$ mice or to two Gy-irradiated WBB6F$_1$-*Kit*^{W}/*Kit*$^{W\text{-}v}$ mice. After bone marrow transplantation, the transplantation of WBB6F$_1$-+/+ CMCs was done as described above within the same day. The irradiation dose of WBB6F$_1$-*Kit*^{W}/*Kit*$^{W\text{-}v}$ mice was reduced because they were remarkably radiosensitive.[27]

Semiquantitative Reverse Transcriptase-Polymerase Chain Reaction (RT-PCR)

Total RNAs were extracted from subcutaneous connective tissue by RNeasy (Qiagen, Hilden, Germany). One μg of total RNA was subjected to reverse transcription by Superscript II (Invitrogen, Carlsbad, CA), and the single-strand cDNA was obtained. Reaction mixture (1, 0.1, or 0.01 μl) was added to 25 μl of PCR mixture containing 1.25 U of *Taq*DNA polymerase (Roche Diagnostics, Mannheim, Germany) and 25 pmol of each of the primers. PCR was performed to amplify the fragment of *KITL*, *MITF*, and *β-actin* genes using the following primers; 5′-AAGACTCGGGCCTACAATGGACAGCCATGG and 5′-CAATGTTGATACGTCCACAATTAC for KITL, 5′-CGCACCCAACAGCCCTATGGCTATGCTCAC and 5′-GGCTGGACAGGAGTTGCTGATGGTAAGGCC for MITF, and 5′-TAAAGACCTCTATGCCAACAC and 5′-CTCCTGCTTGCTGATCCACAT for β-actin.

Immunohistochemistry

The skin sections and the air-bleb membranes were used for immunohistochemical analysis. The skin sections were prepared as described previously.[28] The air-bleb membranes stretched on the glass were fixed in Carnoy's fluid. Samples were incubated sequentially for 10 minutes in methanol containing 0.3% H_2O_2, for 1 hour at room temperature in phosphate-buffered saline containing 2% bovine serum albumin, and then overnight in 1 μg/ml of polyclonal rabbit anti-stem cell factor (SCF) antibody (IBL, Fujioka, Japan). Samples were washed and then incubated for 1 hour in buffer containing biotin-labeled goat anti-rabbit IgG (IBL). Immunoreactions were detected using AEC+ high-sensitivity substrate-chromogen system (DAKO, Carpinteria, CA) according to the manufacturer's instructions.

Statistics

Statistical analysis of data were performed using the Student's *t*-test. Because the number of eosinophils in the air-bleb assay spread widely, a logarithm of each value of infiltrated eosinophils was used for the Student's *t*-test.

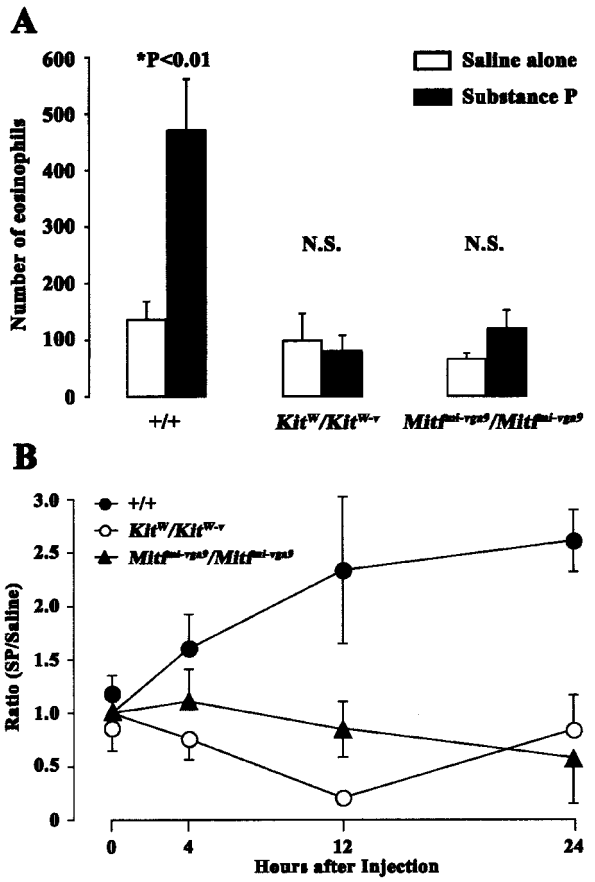

Figure 1. A: Impairment of SP-induced eosinophil infiltration in air-blebs formed in WBB6F$_1$-*Mitf*$^{mi\text{-}vga9}$/*Mitf*$^{mi\text{-}vga9}$ mice. Air-bleb membranes were harvested 4 hours after administration of SP (10^{-5} mol/L). **Open bars**: Number of eosinophils of WBB6F$_1$ mice of indicated genotype administered with saline alone (+/+, $n = 8$; *Kit*^{W}/*Kit*$^{W\text{-}v}$, $n = 8$; *Mitf*$^{mi\text{-}vga9}$/*Mitf*$^{mi\text{-}vga9}$, $n = 11$). **Filled bars**: Mice administered with SP (+/+, $n = 7$; *Kit*^{W}/*Kit*$^{W\text{-}v}$, $n = 8$; *Mitf*$^{mi\text{-}vga9}$/*Mitf*$^{mi\text{-}vga9}$, $n = 7$). The values represent the mean ± SE. *, Compared by *t*-test with the value of mice of the same genotype. N.S., not significant ($P > 0.1$). **B:** Kinetic analysis of SP-induced eosinophil infiltration. The value represents the ratio of the number of infiltrating eosinophils after administration of SP (10^{-5} mol/L) to the mean number of eosinophils after administration of saline alone. **Filled circle**: WBB6F$_1$-+/+ mice administered with SP. **Filled triangle**: WBB6F$_1$-*Kit*^{W}/*Kit*$^{W\text{-}v}$ mice administered with SP. **Open circle**: WBB6F$_1$-*Mitf*$^{mi\text{-}vga9}$/*Mitf*$^{mi\text{-}vga9}$ mice administered with SP. At each time point, 4 to 10 mice were examined, respectively. The values represent the mean ± SE.

Results

Failure of SP-Induced Eosinophil Infiltration in WBB6F$_1$-Mitf$^{mi\text{-}vga9}$/Mitf$^{mi\text{-}vga9}$ Mice

By using the air-bleb assay, we examined the effect of mouse genotype on SP-induced eosinophil infiltration. Saline or saline containing SP was injected into the air-bleb, which was formed by the injection of air at the dorsal skin of WBB6F$_1$-+/+, WBB6F$_1$-*Kit*^{W}/*Kit*$^{W\text{-}v}$, and WBB6F$_1$-*Mitf*$^{mi\text{-}vga9}$/*Mitf*$^{mi\text{-}vga9}$ mice. WBB6F$_1$-+/+ mice and WBB6F$_1$-*Kit*^{W}/*Kit*$^{W\text{-}v}$ mice were used as positive and negative controls, respectively. Administration of SP significantly increased the number of eosinophils in the air-bleb membranes of WBB6F$_1$-+/+ mice (Figure 1A). In contrast, such a significant increase was not observed in WBB6F$_1$-*Kit*^{W}/*Kit*$^{W\text{-}v}$ mice. The increase of infiltrating eosinophils was not observed in WBB6F$_1$-*Mitf*$^{mi\text{-}vga9}$/*Mitf*$^{mi\text{-}vga9}$ mice either (Figure 1A). Neutrophil infiltration after administration of SP was not impaired in *MITF*$^{mi\text{-}vga9}$/*MITF*$^{mi\text{-}vga9}$ mice (data not shown). We next examined the number of infiltrating eosinophils at 12 and 24 hours after administration of SP. The increase of infiltrating eosinophils was not observed in WBB6F$_1$-*Mitf*$^{mi\text{-}vga9}$/*Mitf*$^{mi\text{-}vga9}$ mice at 12 and 24 hours (Figure 1B).

We described that the skin tissue of WBB6F$_1$-*Mitf*$^{mi\text{-}vga9}$/*Mitf*$^{mi\text{-}vga9}$ mice had one third of mast cells compared with the value of WBB6F$_1$-+/+ mice.[12] Unexpectedly, we noticed that mast cells were not present in the air-bleb membranes of WBB6F$_1$-*Mitf*$^{mi\text{-}vga9}$/*Mitf*$^{mi\text{-}vga9}$ mice. To investigate the position of the air-bleb, India ink was injected into the skin instead of air. India ink accumulated in the subcutaneous tissue under panniculus carnosus (Figure 2). This observation revealed that membranes used in the air-bleb assay were composed of subcutaneous connective tissue. In other words, the subcutaneous connective tissue of WBB6F$_1$-*Mitf*$^{mi\text{-}vga9}$/*Mitf*$^{mi\text{-}vga9}$ mice lacked mast cells.

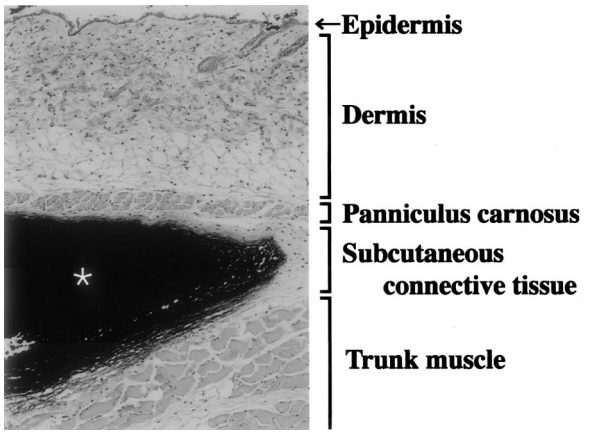

Figure 2. Location of injected India ink (*) at the subcutaneous connective tissue of a WBB6F$_1$-*Mitf*$^{mi\text{-}vga9}$/*Mitf*$^{mi\text{-}vga9}$ mouse.

We examined the number of mast cells in the dermis (between epidermis and panniculus carnosus) and in the subcutaneous connective tissue (air-bleb membrane) of WBB6F$_1$-+/+ and WBB6F$_1$-*Mitf*$^{mi\text{-}vga9}$/*Mitf*$^{mi\text{-}vga9}$ mice of different ages. The number of mast cells in the dermis was comparable between WBB6F$_1$-+/+ and WBB6F$_1$-*Mitf*$^{mi\text{-}vga9}$/*Mitf*$^{mi\text{-}vga9}$ mice at 3 weeks after birth. At 15 and 28 weeks after birth, however, the number of mast cells in the dermis of WBB6F$_1$-*Mitf*$^{mi\text{-}vga9}$/*Mitf*$^{mi\text{-}vga9}$ mice was significantly smaller than that of WBB6F$_1$-+/+ mice (Figure 3A). The number of mast cells increased with age in subcutaneous connective tissue of WBB6F$_1$-+/+ mice. In contrast, mast cells did not develop in the subcutaneous connective tissue of WBB6F$_1$-*Mitf*$^{mi\text{-}vga9}$/*Mitf*$^{mi\text{-}vga9}$ mice at all ages examined in the present study (Figure 3B).

Effect of Transplantation of CMCs

The lack of mast cells appeared to cause the failure of SP-induced eosinophil infiltration in the air-bleb membranes of WBB6F$_1$-*Mitf*$^{mi\text{-}vga9}$/*Mitf*$^{mi\text{-}vga9}$ mice. We injected WBB6F$_1$-+/+ CMCs subcutaneously to reconsti-

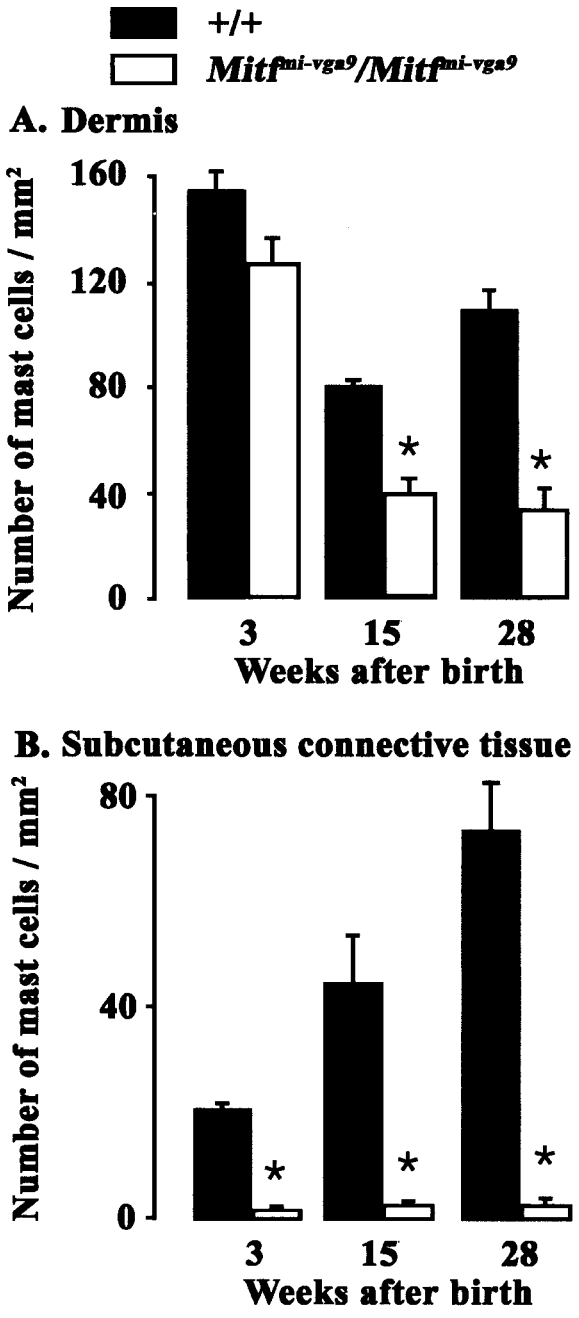

Figure 3. Number of mast cells in the dermis (**A**) and air-bleb membranes (**B**) of WBB6F$_1$-+/+ and WBB6F$_1$-*Mitf* $^{mi\text{-}vga9}$/*Mitf* $^{mi\text{-}vga9}$ mice of various ages. Each bar indicates mean ± SE of 5 to 17 mice. *, $P < 0.01$ by *t*-test when compared with the value of WBB6F$_1$-+/+ mice of the same age.

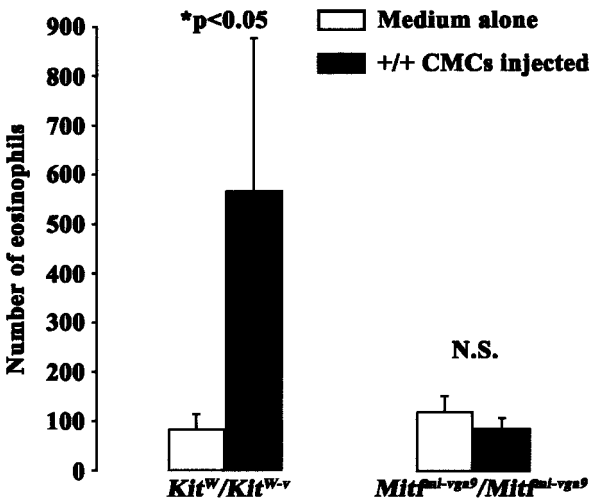

Figure 4. Effect of prior transplantation of WBB6F$_1$-+/+ CMCs on eosinophil infiltration induced by SP. Six weeks after injection of medium alone or WBB6F$_1$-+/+ CMCs to WBB6F$_1$-*Kit*^{W}/*Kit*$^{W\text{-}v}$ and WBB6F$_1$-*Mitf* $^{mi\text{-}vga9}$/*Mitf* $^{mi\text{-}vga9}$ mice, air-blebs were formed at the injection sites. Number of infiltrating eosinophils was examined 4 hours after the administration of SP. Each bar indicates mean ± SE of six to seven mice. *, Compared by *t*-test with the value of mice of the same genotype. N.S., not significant ($P > 0.2$).

tute mast cell depletion of WBB6F$_1$-*Mitf* $^{mi\text{-}vga9}$/*Mitf* $^{mi\text{-}vga9}$ mice. WBB6F$_1$-*Kit*^{W}/*Kit*$^{W\text{-}v}$ mice were used as control recipients, because their mast cell deficiency and failure of SP-induced eosinophil infiltration were normalized by the subcutaneous injection of WBB6F$_1$-+/+ CMCs.[22] Although WBB6F$_1$-+/+ CMCs survived in the subcutaneous connective tissue of not only WBB6F$_1$-*Kit*^{W}/*Kit*$^{W\text{-}v}$ mice but also WBB6F$_1$-*Mitf* $^{mi\text{-}vga9}$/*Mitf* $^{mi\text{-}vga9}$ mice, the CMC injection did not increase the number of infiltrating eosinophils induced by SP in the subcutaneous connective tissue of WBB6F$_1$-*Mitf* $^{mi\text{-}vga9}$/*Mitf* $^{mi\text{-}vga9}$ mice (Figure 4).

There are possibilities that eosinophils of WBB6F$_1$-*Mitf* $^{mi\text{-}vga9}$/*Mitf* $^{mi\text{-}vga9}$ mice have abnormalities. First, we examined the number of eosinophils in peripheral blood of WBB6F$_1$-+/+, WBB6F$_1$-*Kit*^{W}/*Kit*$^{W\text{-}v}$, and WBB6F$_1$-*Mitf* $^{mi\text{-}vga9}$/*Mitf* $^{mi\text{-}vga9}$ mice. The proportion of eosinophils in WBB6F$_1$-*Kit*^{W}/*Kit*$^{W\text{-}v}$ mice was significantly smaller than that of WBB6F$_1$-+/+ mice, and the proportion in WBB6F$_1$-*Mitf* $^{mi\text{-}vga9}$/*Mitf* $^{mi\text{-}vga9}$ mice was comparable with that of WBB6F$_1$-+/+ mice (Table 1).

Next, the chemotactic potential of WBB6F$_1$-*Mitf* $^{mi\text{-}vga9}$/*Mitf* $^{mi\text{-}vga9}$ eosinophils was examined. Because LTB_4 is a potent eosinophil chemoattractant[29] and is contained by mast cells,[30,31] we injected LTB_4 into air-blebs formed in the back of WBB6F$_1$-+/+, WBB6F$_1$-*Kit*^{W}/*Kit*$^{W\text{-}v}$, and WBB6F$_1$-*Mitf* $^{mi\text{-}vga9}$/*Mitf* $^{mi\text{-}vga9}$ mice. LTB_4 induced the eosinophil infiltration in all WBB6F$_1$-+/+, WBB6F$_1$-*Kit*^{W}/*Kit*$^{W\text{-}v}$, and WBB6F$_1$-*Mitf* $^{mi\text{-}vga9}$/*Mitf* $^{mi\text{-}vga9}$ mice (Figure 5). No significant differences were observed among mice of different genotypes.

Eosinophils in the blood of WBB6F$_1$-*Mitf* $^{mi\text{-}vga9}$/*Mitf* $^{mi\text{-}vga9}$ mice were exchanged to those of WBB6F$_1$-+/+ mouse origin by the bone marrow transplantation. Because the number of mast cells in the subcutaneous connective tissue of WBB6F$_1$-*Mitf* $^{mi\text{-}vga9}$/*Mitf* $^{mi\text{-}vga9}$ recipients remained in low levels after the bone marrow transplanta-

Table 1. Proportion of Eosinophils in Peripheral Blood Leukocytes of WBB6F1-+/+ Mice of Various Genotypes

Genotype	No. of mice	Eosinophils/ leukocytes (%)*
+/+	8	2.9 ± 0.3
Kit^W/*Kit*$^{W\text{-}v}$	8	1.4 ± 0.3†
Mitf $^{mi\text{-}vga9}$/*Mitf* $^{mi\text{-}vga9}$	8	3.1 ± 0.4

*Mean ± SE.
$^\dagger P < 0.01$, when compared to the value of WBB6F$_1$-+/+ mice.

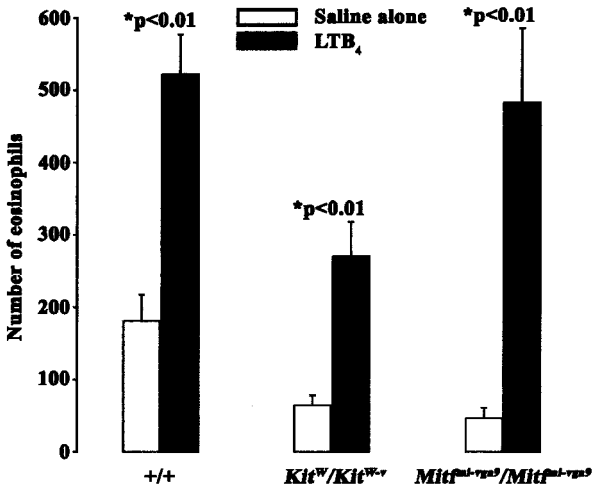

Figure 5. Effect of LTB_4 (300 ng/ml) administration on numbers of eosinophils in the air-bleb membranes formed in $WBB6F_1$ mice of various genotypes. Each bar indicates mean ± SE of seven to eight mice. *, Compared by *t*-test with $WBB6F_1$ mice of the same genotype administered with saline alone.

tion, $WBB6F_1$-+/+ CMCs were also injected into the skin of the $WBB6F_1$-*Mitf*$^{mi\text{-}vga9}$/*Mitf*$^{mi\text{-}vga9}$ recipients. Six weeks after the bone marrow transplantation and CMC injection, the SP-induced eosinophil infiltration was examined. The number of infiltrating eosinophils in the air-bleb membranes of the $WBB6F_1$-*Mitf*$^{mi\text{-}vga9}$/*Mitf*$^{mi\text{-}vga9}$ recipients was not significantly increased by the bone marrow transplantation and CMC injection (data not shown).

Distribution of Transplanted CMCs

The impaired eosinophil infiltration observed in $WBB6F_1$-*Mitf*$^{mi\text{-}vga9}$/*Mitf*$^{mi\text{-}vga9}$ mice did not appear to be caused by the abnormal function of eosinophils of these mutant mice. The impairment was normalized by the subcutaneous injection of $WBB6F_1$-+/+ CMCs in $WBB6F_1$-*Kit*^{W}/*Kit*$^{W\text{-}v}$ mice but not in $WBB6F_1$-*Mitf*$^{mi\text{-}vga9}$/*Mitf*$^{mi\text{-}vga9}$ mice, indicating that injected $WBB6F_1$-+/+ CMCs did function in the subcutaneous tissue of $WBB6F_1$-*Kit*^{W}/*Kit*$^{W\text{-}v}$ mice but not in that of $WBB6F_1$-*Mitf*$^{mi\text{-}vga9}$/*Mitf*$^{mi\text{-}vga9}$ mice.

We compared the number and distribution pattern of mast cells in air-bleb membranes of intact $WBB6F_1$-+/+ mice, $WBB6F_1$-+/+ CMC-injected, or $WBB6F_1$-*Mitf*$^{mi\text{-}vga9}$/*Mitf*$^{mi\text{-}vga9}$ CMC-injected $WBB6F_1$-*Kit*^{W}/*Kit*$^{W\text{-}v}$ mice, and $WBB6F_1$-+/+ CMC-injected or $WBB6F_1$-*Mitf*$^{mi\text{-}vga9}$/*Mitf*$^{mi\text{-}vga9}$ CMC-injected $WBB6F_1$-*Mitf*$^{mi\text{-}vga9}$/*Mitf*$^{mi\text{-}vga9}$ mice (Table 2). $WBB6F_1$-+/+ CMCs survived in the subcutaneous connective tissue of $WBB6F_1$-*Mitf*$^{mi\text{-}vga9}$/*Mitf*$^{mi\text{-}vga9}$ mice, but $WBB6F_1$-*Mitf*$^{mi\text{-}vga9}$/*Mitf*$^{mi\text{-}vga9}$ CMCs did not. $WBB6F_1$-*Mitf*$^{mi\text{-}vga9}$/*Mitf*$^{mi\text{-}vga9}$ CMCs did survive in the subcutaneous connective tissue of $WBB6F_1$-*Kit*^{W}/*Kit*$^{W\text{-}v}$ mice, but the mean number of mast cells was nine times greater when $WBB6F_1$-+/+ CMCs were injected than when $WBB6F_1$-*Mitf*$^{mi\text{-}vga9}$/*Mitf*$^{mi\text{-}vga9}$ CMCs were injected (Table 2). The mean number of mast cells was comparable between air-bleb membranes of intact $WBB6F_1$-+/+ mice and those of $WBB6F_1$-*Mitf*$^{mi\text{-}vga9}$/*Mitf*$^{mi\text{-}vga9}$ mice injected with $WBB6F_1$-+/+ CMCs. On the other hand, the mean number of mast cells was two times greater in air-bleb membranes of $WBB6F_1$-*Kit*^{W}/*Kit*$^{W\text{-}v}$ mice injected with $WBB6F_1$-+/+ CMCs than in those of intact $WBB6F_1$-+/+ mice (Table 2).

In the air-bleb membranes formed in $WBB6F_1$-+/+ mice, ≥10 mast cells were detected in most of the high-power fields. Therefore, the proportion of such high-power fields containing ≥10 mast cells was used as an index of mast cell distribution. The proportion was significantly greater in intact $WBB6F_1$-+/+ mice than in $WBB6F_1$-+/+ CMC-injected $WBB6F_1$-*Kit*^{W}/*Kit*$^{W\text{-}v}$ mice. And the proportion was significantly greater in $WBB6F_1$-+/+ CMC-injected $WBB6F_1$-*Kit*^{W}/*Kit*$^{W\text{-}v}$ mice than in $WBB6F_1$-+/+ CMC-injected $WBB6F_1$-*Mitf*$^{mi\text{-}vga9}$/*Mitf*$^{mi\text{-}vga9}$ mice (Table 2).

Air-bleb membranes of intact $WBB6F_1$-+/+ mice and those of $WBB6F_1$-+/+ CMC-injected $WBB6F_1$-*Kit*^{W}/*Kit*$^{W\text{-}v}$ and $WBB6F_1$-*Mitf*$^{mi\text{-}vga9}$/*Mitf*$^{mi\text{-}vga9}$ mice were stained with berberine sulfate. Most mast cells were stained with berberine sulfate in the air-bleb membranes of intact $WBB6F_1$-+/+ and $WBB6F_1$-+/+ CMC-injected $WBB6F_1$-*Kit*^{W}/*Kit*$^{W\text{-}v}$ and $WBB6F_1$-*Mitf*$^{mi\text{-}vga9}$/*Mitf*$^{mi\text{-}vga9}$ mice, suggesting that injected $WBB6F_1$-+/+ CMCs acquired the phenotype of connective tissue-type mast cells in the subcutaneous connective tissue of not only $WBB6F_1$-*Kit*^{W}/*Kit*$^{W\text{-}v}$ mice but also $WBB6F_1$-*Mitf*$^{mi\text{-}vga9}$/*Mitf*$^{mi\text{-}vga9}$ mice (Figure 6). Mast cells in the subcutaneous connec-

Table 2. Number and Distribution of Mast Cells in Air-Bleb Membranes of $WBB6F_1$ Mice of Various Genotypes 6 Weeks after Subcutaneous Transplantation of CMCs

Genotype			No. of mast cells in air-bleb membranes (per 10 mm^2)*	Proportion of fields containing >10 mast cells (%)*
Donor	Recipient	No. of mice		
None	+/+	9	595 ± 88†	91 ± 5†‡
None	*Mitf*$^{mi\text{-}vga9}$/*Mitf*$^{mi\text{-}vga9}$	8	< 1†‡§	0†‡§
Mitf$^{mi\text{-}vga9}$/*Mitf*$^{mi\text{-}vga9}$	*Mitf*$^{mi\text{-}vga9}$/*Mitf*$^{mi\text{-}vga9}$	8	< 1†‡§	0†‡§
+/+	*Mitf*$^{mi\text{-}vga9}$/*Mitf*$^{mi\text{-}vga9}$	7	457 ± 49†	24 ± 5†§
None	*Kit*^{W}/*Kit*$^{W\text{-}v}$	8	0†‡§	0†‡§
Mitf$^{mi\text{-}vga9}$/*Mitf*$^{mi\text{-}vga9}$	*Kit*^{W}/*Kit*$^{W\text{-}v}$	6	131 ± 59†‡§	13 ± 3†§
+/+	*Kit*^{W}/*Kit*$^{W\text{-}v}$	9	1184 ± 160‡§	47 ± 6‡§

*Mean ± SE.
$^{\dagger}P < 0.01$, when compared to the value observed in $WBB6F_1$-*Kit*^{W}/*Kit*$^{W\text{-}v}$ mice that received transplantation of $WBB6F_1$-+/+ CMCs.
$^{\ddagger}P < 0.01$, when compared to the value observed in $WBB6F_1$-*Mitf*$^{mi\text{-}vga9}$/*Mitf*$^{mi\text{-}vga9}$ mice that received transplantation of $WBB6F_1$-+/+ CMCs.
$^{\S}P < 0.01$, when compared to the value observed in intact $WBB6F_1$-+/+ mice.

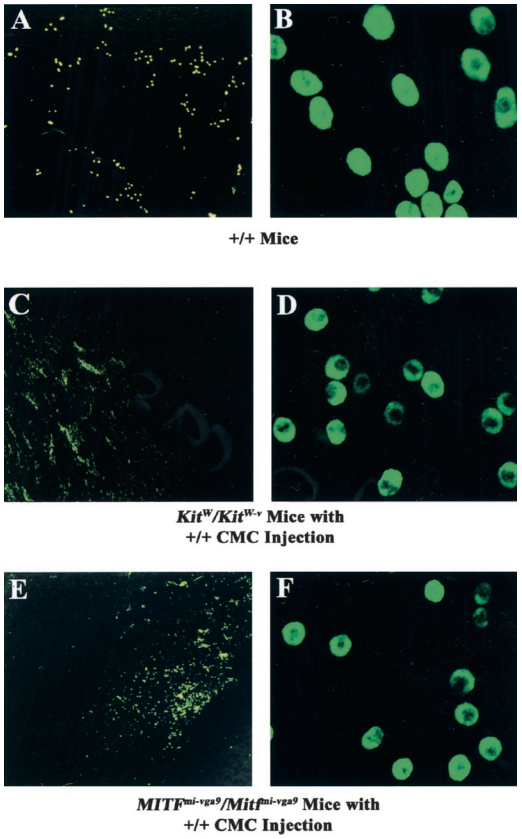

Figure 6. Fluorescent microscopic images of air-bleb membranes formed in various WBB6F$_1$ mice stained with berberine sulfate. **A** and **B:** Intact WBB6F$_1$-+/+ mice. **C** and **D:** WBB6F$_1$-*Kit^W/Kit^{W-v}* mice injected with WBB6F$_1$-+/+ CMCs. **E** and **F:** WBB6F$_1$-*Mitf$^{mi-vga9}$/Mitf$^{mi-vga9}$* injected with WBB6F$_1$-+/+ CMCs. **A**, **C**, and **E:** Distribution of mast cells. **B**, **D**, and **F:** Images used to determine cellular area and fluorescence intensity. Original magnifications: ×40 (**A**, **C**, **E**); ×800 (**B**, **D**, **F**).

tive tissue of intact WBB6F$_1$-+/+ mice showed a dispersed distribution pattern, whereas those of rescued WBB6F$_1$-*Kit^W/Kit^{W-v}* and WBB6F$_1$-*Mitf$^{mi-vga9}$/Mitf$^{mi-vga9}$* mice did not show such a dispersed distribution pattern. Injected WBB6F$_1$-+/+ CMCs formed clusters in the subcutaneous tissue of WBB6F$_1$-*Kit^W/Kit^{W-v}* and WBB6F$_1$-*Mitf$^{mi-vga9}$/Mitf$^{mi-vga9}$* mice (Figure 6). The clusters were larger in WBB6F$_1$-*Kit^W/Kit^{W-v}* mice than in WBB6F$_1$-*Mitf$^{mi-vga9}$/Mitf$^{mi-vga9}$* mice. As a result, the areas with normally distributed mast cells, as observed in intact WBB6F$_1$-+/+ mice, were apparently less in WBB6F$_1$-+/+ CMC-injected WBB6F$_1$-*Mitf$^{mi-vga9}$/Mitf$^{mi-vga9}$* mice than in WBB6F$_1$-+/+ CMC-injected WBB6F$_1$-*Kit^W/Kit^{W-v}* mice (Figure 6).

To assess the maturation of WBB6F$_1$-+/+ CMCs that were injected in the subcutaneous connective tissue, we measured a cellular area and a fluorescent intensity. The cellular area may represent the cell volume in stretched specimens, and the fluorescent intensity the content of heparin. Cellular area of individual mast cells in air-bleb membranes of intact WBB6F$_1$-+/+ mice was larger than that of individual mast cells in air-bleb membranes of WBB6F$_1$-+/+ CMC-injected WBB6F$_1$-*Kit^W/Kit^{W-v}* and WBB6F$_1$-*Mitf$^{mi-vga9}$/Mitf$^{mi-vga9}$* mice (Figure 6, Table 3). No significant difference was detectable between mast cells developing in WBB6F$_1$-*Kit^W/Kit^{W-v}* mice and those developing in WBB6F$_1$-*Mitf$^{mi-vga9}$/Mitf$^{mi-vga9}$* mice. Fluorescent intensity of individual mast cells was compared among intact WBB6F$_1$-+/+ mice, WBB6F$_1$-+/+ CMC-injected WBB6F$_1$-*Kit^W/Kit^{W-v}* mice, and WBB6F$_1$-+/+ CMC-injected WBB6F$_1$-*Mitf$^{mi-vga9}$/Mitf$^{mi-vga9}$* mice. The fluorescent intensity was higher in mast cells of intact WBB6F$_1$-+/+ mice than in those of WBB6F$_1$-+/+ CMC-injected WBB6F$_1$-*Kit^W/Kit^{W-v}* and WBB6F$_1$-*Mitf$^{mi-vga9}$/Mitf$^{mi-vga9}$* mice. No significant difference was detectable between mast cells developing in WBB6F$_1$-*Kit^W/Kit^{W-v}* mice and those developing in WBB6F$_1$-*Mitf$^{mi-vga9}$/Mitf$^{mi-vga9}$* mice (Table 3).

To assess whether abnormal distribution of mast cells in CMC-injected WBB6F$_1$-*Mitf$^{mi-vga9}$/Mitf$^{mi-vga9}$* mice may be attributable to the abnormality of KITL expression in the subcutaneous connective tissue, we compared the amount of KITL mRNA among the subcutaneous connective tissue of WBB6F$_1$-+/+, WBB6F$_1$-*Kit^W/Kit^{W-v}*, and WBB6F$_1$-*Mitf$^{mi-vga9}$/Mitf$^{mi-vga9}$* mice by semiquantitative RT-PCR. No significant difference was observed in KITL transcription level (Figure 7). To detect KITL in a protein level and to assess the distribution of KITL-expressing cells, we performed the immunohistochemical analysis using subcutaneous connective tissue. Although the hair bulbs of dermis were strongly stained, no detectable signals were observed in the subcutaneous connective tissues of WBB6F$_1$-+/+, WBB6F$_1$-*Kit^W/Kit^{W-v}*, and WBB6F$_1$-*Mitf$^{mi-vga9}$/Mitf$^{mi-vga9}$* mice (data not shown). There is a possibility that tissues of mice of WBB6F$_1$-*Mitf$^{mi-vga9}$/Mitf$^{mi-vga9}$* genotype have a defect in microenvironment that is necessary for the migration and settlement of normal CMCs. We examined whether MITF was expressed in the subcutaneous connective tissue of WBB6F$_1$-+/+, WBB6F$_1$-*Kit^W/Kit^{W-v}*, and WBB6F$_1$-*Mitf$^{mi-vga9}$/*

Table 3. Cellular Area and Fluorescent Intensity of Mast Cells in Subcutaneous Connective Tissue of WBB6F$_1$ Mice of Various Genotypes 6 Weeks after Subcutaneous Transplantation of CMCs

Genotype				
Donor	Recipient	No. of mast cells examined	Cellular area (μm^2)*	Fluorescent intensity*†
None	+/+	65	122.4 ± 4.9	476 ± 21
+/+	*Kit^W/Kit^{W-v}*	121	83.4 ± 1.7‡	265 ± 10‡
+/+	*Mitf$^{mi-vga9}$/Mitf$^{mi-vga9}$*	109	84.6 ± 2.2‡	255 ± 11‡

*Mean ± SE.
†Integrated fluorescent intensity per cell shown by arbitrary unit.
‡$P < 0.01$, when compared to the value observed in WBB6F$_1$-+/+ mice that received transplantation of WBB6F$_1$-+/+ CMCs.

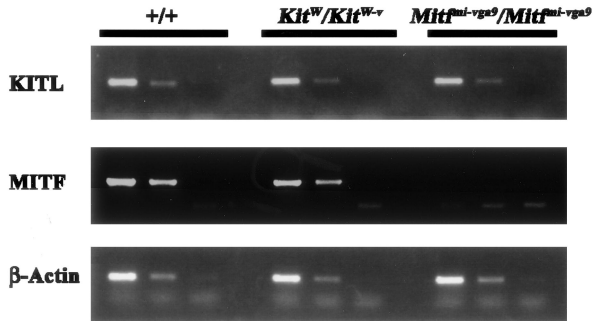

Figure 7. Expression levels of KITL and MITF mRNA in the subcutaneous connective tissue of intact WBB6F$_1$-+/+, WBB6F$_1$-*Kit^W/Kit^{W-v}*, and WBB6F$_1$-*Mitf$^{mi\text{-}vga9}$/Mitf$^{mi\text{-}vga9}$* mice. Semiquantitative RT-PCR was done to compare the expression levels of KITL, MITF, and β-actin mRNAs. RNA extracted from subcutaneous connective tissue of intact WBB6F$_1$-+/+, WBB6F$_1$-*Kit^W/Kit^{W-v}*, and WBB6F$_1$-*Mitf$^{mi\text{-}vga9}$/Mitf$^{mi\text{-}vga9}$* mice was subjected to RT-PCR. The volume of reverse-transcribed product used as a template was 1 μl (**left**), 0.1 μl (**middle**), and 0.01 μl (**right**), respectively.

Mitf$^{mi\text{-}vga9}$ mice. The expression of MITF mRNA was detectable in the subcutaneous connective tissue of intact WBB6F$_1$-+/+ and WBB6F$_1$-*Kit^W/Kit^{W-v}* mice, but did not in those tissues of intact WBB6F$_1$-*Mitf$^{mi\text{-}vga9}$/Mitf$^{mi\text{-}vga9}$* mice (Figure 7).

Discussion

Although a decreased number of mast cells (one third that of WBB6F$_1$-+/+ mice) was present in the dermis of WBB6F$_1$-*Mitf$^{mi\text{-}vga9}$/Mitf$^{mi\text{-}vga9}$* mice, their subcutaneous connective tissue lacked mast cells. We have reported the lack of mast cells in the lung, spleen, stomach, and peritoneal cavity of WBB6F$_1$-*Mitf$^{mi\text{-}vga9}$/Mitf$^{mi\text{-}vga9}$* mice.[18] Therefore, the dermis is an exceptional tissue, and the subcutaneous connective tissue has a common characteristic with other tissues. The dermis is also exceptional in another viewpoint of mast cell development; mast cells develop before birth in the dermis[32] but after birth in other tissues. MITF appears to be essential for development of mast cells after birth in tissues other than the dermis.

When CMCs of WBB6F$_1$-+/+ and WBB6F$_1$-*Mitf$^{mi\text{-}vga9}$/Mitf$^{mi\text{-}vga9}$* mice were transplanted to the subcutaneous connective tissue of WBB6F$_1$-*Mitf$^{mi\text{-}vga9}$/Mitf$^{mi\text{-}vga9}$* mice, WBB6F$_1$-+/+ CMCs but not WBB6F$_1$-*Mitf$^{mi\text{-}vga9}$/Mitf$^{mi\text{-}vga9}$* CMCs survived. Even if mast cell precursors of WBB6F$_1$-*Mitf$^{mi\text{-}vga9}$/Mitf$^{mi\text{-}vga9}$* mice arrive at their subcutaneous connective tissue, they may not be recognized as differentiated mast cells. When WBB6F$_1$-+/+ CMCs and WBB6F$_1$-*Mitf$^{mi\text{-}vga9}$/Mitf$^{mi\text{-}vga9}$* CMCs were transplanted to the subcutaneous connective tissue of WBB6F$_1$-*Kit^W/Kit^{W-v}* mice, mast cells were detected in both cases. However, the number of mast cells was nine times greater when WBB6F$_1$-+/+ CMCs were transplanted than when WBB6F$_1$-*Mitf$^{mi\text{-}vga9}$/Mitf$^{mi\text{-}vga9}$* CMCs were transplanted. These showed that molecules expressed in WBB6F$_1$-+/+ CMCs but not in WBB6F$_1$-*Mitf$^{mi\text{-}vga9}$/Mitf$^{mi\text{-}vga9}$* CMCs were important for the survival and differentiation in the subcutaneous tissues. Recently, we found that spermatogenic immunoglobulin superfamily (SgIGSF) that was expressed in WBB6F$_1$-+/+ CMCs but not WBB6F$_1$-*Mitf$^{mi\text{-}vga9}$/Mitf$^{mi\text{-}vga9}$* CMCs mediated the adhesion between mast cells and fibroblasts. Then, we examined the survival of WBB6F$_1$-*Mitf$^{mi\text{-}vga9}$/Mitf$^{mi\text{-}vga9}$* CMCs overexpressing SgIGSF in the peritoneal cavity of WBB6F$_1$-*Mitf$^{mi\text{-}vga9}$/Mitf$^{mi\text{-}vga9}$* mice. The survival of WBB6F$_1$-*Mitf$^{mi\text{-}vga9}$/Mitf$^{mi\text{-}vga9}$* CMCs was partially but not completely rescued by the overexpression of SgIGSF (Ito et al, manuscript submitted). This suggested that other molecules that support the function of SgIGSF might participate in the survival of mast cells.

The transplanted WBB6F$_1$-*Mitf$^{mi\text{-}vga9}$/Mitf$^{mi\text{-}vga9}$* CMCs differentiate in the subcutaneous connective tissue of WBB6F$_1$-*Kit^W/Kit^{W-v}* mice but not WBB6F$_1$-*Mitf$^{mi\text{-}vga9}$/Mitf$^{mi\text{-}vga9}$* mice. The subcutaneous connective tissue of WBB6F$_1$-*Kit^W/Kit^{W-v}* mice was more appropriate for survival and/or differentiation of WBB6F$_1$-*Mitf$^{mi\text{-}vga9}$/Mitf$^{mi\text{-}vga9}$* CMCs than the subcutaneous connective tissue of WBB6F$_1$-*Mitf$^{mi\text{-}vga9}$/Mitf$^{mi\text{-}vga9}$* mice. This is consistent with the fact that the number of mast cells was two times greater when WBB6F$_1$-+/+ CMCs were transplanted to the subcutaneous connective tissue of WBB6F$_1$-*Kit^W/Kit^{W-v}* mice than when they were transplanted in the subcutaneous connective tissue of WBB6F$_1$-*Mitf$^{mi\text{-}vga9}$/Mitf$^{mi\text{-}vga9}$* mice. The subcutaneous connective tissue of WBB6F$_1$-*Kit^W/Kit^{W-v}* mice appeared to be a better environment for survival and/or differentiation of not only WBB6F$_1$-*Mitf$^{mi\text{-}vga9}$/Mitf$^{mi\text{-}vga9}$* CMCs but also WBB6F$_1$-+/+ CMCs. There are some explanations for this. The dermis of WBB6F$_1$-*Kit^W/Kit^{W-v}* mice practically lacked mast cells whereas the dermis of WBB6F$_1$-*Mitf$^{mi\text{-}vga9}$/Mitf$^{mi\text{-}vga9}$* mice contained the decreased but appreciable number of mast cells. Because mast cells express KIT, the concentration of KITL may be greater in WBB6F$_1$-*Kit^W/Kit^{W-v}* mice than in WBB6F$_1$-*Mitf$^{mi\text{-}vga9}$/Mitf$^{mi\text{-}vga9}$* mice. We attempted to detect KITL protein in the subcutaneous tissues with the immunohistochemistry. Although the expression of KITL in the hair bulbs was detected as described by Peters and colleagues,[34] it was not detectable in the subcutaneous connective tissues. Mature mast cells may inhibit development of mast cells from their precursors.[35] Mast cells that are present in the dermis of WBB6F$_1$-*Mitf$^{mi\text{-}vga9}$/Mitf$^{mi\text{-}vga9}$* mice might inhibit development of mast cells in their subcutaneous connective tissue.

Administration of SP induced eosinophil infiltration in air-blebs of WBB6F$_1$-+/+ mice but not in those of WBB6F$_1$-*Kit^W/Kit^{W-v}* mice as reported by Matsuda and colleagues.[22] The deficient eosinophil infiltration was normalized by transplantation of WBB6F$_1$-+/+ CMCs. Although the deficiency in eosinophil infiltration was observed in WBB6F$_1$-*Mitf$^{mi\text{-}vga9}$/Mitf$^{mi\text{-}vga9}$* mice as well, the deficiency of WBB6F$_1$-*Mitf$^{mi\text{-}vga9}$/Mitf$^{mi\text{-}vga9}$* mice was not normalized by the transplantation of WBB6F$_1$-+/+ CMCs. The deficient eosinophil infiltration was not attributable to defects of eosinophils of WBB6F$_1$-*Mitf$^{mi\text{-}vga9}$/Mitf$^{mi\text{-}vga9}$* mouse origin because of the following two reasons. Eosinophils of WBB6F$_1$-+/+ mouse origin did not infiltrate in air blebs formed in WBB6F$_1$-*Mitf$^{mi\text{-}vga9}$/Mitf$^{mi\text{-}vga9}$* mice that had received transplantation of both WBB6F$_1$-+/+ bone marrow cells and CMCs. Eosinophils

of WBB6F$_1$-*Mitf$^{mi\text{-}vga9}$/Mitf$^{mi\text{-}vga9}$* mice can infiltrate in air-blebs formed in the back of WBB6F$_1$-*Mitf$^{mi\text{-}vga9}$/Mitf$^{mi\text{-}vga9}$* mice after administration of LTB_4.

Transplantation of WBB6F$_1$-+/+ CMCs normalized SP-induced eosinophil infiltration in WBB6F$_1$-*Kit^{W}/Kit$^{W\text{-}v}$* mice but not in WBB6F$_1$-*Mitf$^{mi\text{-}vga9}$/Mitf$^{mi\text{-}vga9}$* mice. WBB6F$_1$-+/+ CMCs showed comparable cellular area and fluorescent intensity in subcutaneous connective tissue of WBB6F$_1$-*Kit^{W}/Kit$^{W\text{-}v}$* mice and in that of WBB6F$_1$-*Mitf$^{mi\text{-}vga9}$/Mitf$^{mi\text{-}vga9}$* mice. The greater number of mast cells that appeared in the subcutaneous connective tissue of WBB6F$_1$-*Kit^{W}/Kit$^{W\text{-}v}$* mice after transplantation of WBB6F$_1$-+/+ CMCs may explain the difference. Another explanation was the different cluster pattern of injected WBB6F$_1$-+/+ CMCs between WBB6F$_1$-*Kit^{W}/Kit$^{W\text{-}v}$* mice and WBB6F$_1$-*Mitf$^{mi\text{-}vga9}$/Mitf$^{mi\text{-}vga9}$* mice. When we counted at random 10 high-power fields of air-bleb membrane injected with WBB6F$_1$-+/+ CMCs, the proportion of fields containing no or few mast cells (less than 10 mast cells) was significantly higher in WBB6F$_1$-*Mitf$^{mi\text{-}vga9}$/Mitf$^{mi\text{-}vga9}$* mice than in WBB6F$_1$-*Kit^{W}/Kit$^{W\text{-}v}$* mice. The microenvironment supporting growth of mast cells may be deficient in WBB6F$_1$-*Mitf$^{mi\text{-}vga9}$/Mitf$^{mi\text{-}vga9}$* mice. In fact, we recently reported that the microenvironment of WBB6F$_1$-*Mitf$^{mi\text{-}vga9}$/Mitf$^{mi\text{-}vga9}$* mice was not suitable for growth of mast cells as compared to that of WBB6F$_1$-*Kit^{W}/Kit$^{W\text{-}v}$* mice by using bone marrow and skin transplantations.[36] The deficient microenvironment of WBB6F$_1$-*Mitf$^{mi\text{-}vga9}$/Mitf$^{mi\text{-}vga9}$* mice may cause the insufficient distribution of injected WBB6F$_1$-+/+ CMCs, and result in the deficient eosinophil infiltration.

We recently reported a comparable observation in the peritoneal cavity of WBB6F$_1$-*Kit^{W}/Kit$^{W\text{-}v}$* and WBB6F$_1$-*Mitf$^{mi\text{-}vga9}$/Mitf$^{mi\text{-}vga9}$* mice.[18] The proportion of death from acute septic peritonitis, which was induced by cecal ligation and puncture, was higher in WBB6F$_1$-*Kit^{W}/Kit$^{W\text{-}v}$* mice and WBB6F$_1$-*Mitf$^{mi\text{-}vga9}$/Mitf$^{mi\text{-}vga9}$* mice than in WBB6F$_1$-+/+ mice. The higher mortality was normalized by the prior intraperitoneal transplantation of WBB6F$_1$-+/+ CMCs in WBB6F$_1$-*Kit^{W}/Kit$^{W\text{-}v}$* mice but not in WBB6F$_1$-*Mitf$^{mi\text{-}vga9}$/Mitf$^{mi\text{-}vga9}$* mice. WBB6F$_1$-+/+ CMCs settled not only in the peritoneal cavity but also in the mesentery of WBB6F$_1$-*Kit^{W}/Kit$^{W\text{-}v}$* mice, but WBB6F$_1$-+/+ CMCs settled only in the peritoneal cavity of WBB6F$_1$-*Mitf$^{mi\text{-}vga9}$/Mitf$^{mi\text{-}vga9}$* mice. Because effective neutrophil infiltration occurred only in the rescued WBB6F$_1$-*Kit^{W}/Kit$^{W\text{-}v}$* mice, the appropriate anatomical distribution of transplanted WBB6F$_1$-+/+ CMCs appeared to be necessary for the neutrophil infiltration.[18] The neutrophil infiltration, which may be induced by tumor necrosis factor-α released by mast cells, is considered to be essential for the defense mechanism against the acute bacterial peritonitis.[37,38] Mast cells settled in the mesentery may secrete tumor necrosis factor-α and mediate neutrophil recruitment more efficiently than those settled in the peritoneal cavity, because the probability of localization in the vicinity of blood vessels may be higher in the former than in the latter. The greater number and/or the more dispersed distribution of injected WBB6F$_1$-+/+ CMCs might increase the probability of localization in the vicinity of blood vessels of subcutaneous connective tissues, and might normalize SP-induced eosinophil infiltration in WBB6F$_1$-*Kit^{W}/Kit$^{W\text{-}v}$* mice.

Taken together, WBB6F$_1$-*Mitf$^{mi\text{-}vga9}$/Mitf$^{mi\text{-}vga9}$* mice are useful as the third mast cell-deficient mice. The comparison between WBB6F$_1$-+/+ CMC-transplanted WBB6F$_1$-*Kit^{W}/Kit$^{W\text{-}v}$* mice and WBB6F$_1$-+/+ CMC-transplanted WBB6F$_1$-*Mitf$^{mi\text{-}vga9}$/Mitf$^{mi\text{-}vga9}$* mice may give insights on relationship between anatomical distribution of mast cells and their physiological functions.

Acknowledgments

We thank Dr. Heinz Arnheiter (National Institutes of Health, Bethesda, MD) for providing us with the original stock of *Mitf$^{mi\text{-}vga9}$/Mitf$^{mi\text{-}vga9}$* mice; and C. Murakami, T. Sawamura, K. Hashimoto, and M. Kohara for technical assistance.

References

1. Kitamura Y, Go S, Hatanaka K: Decrease of mast cells in W/Wv mice and their increase by bone marrow transplantation. Blood 1978, 52:447–452
2. Kitamura Y, Go S: Decreased production of mast cells in S1/S1d anemic mice. Blood 1979, 53:492–497
3. Stechschulte DJ, Sharma R, Dileepan KN, Simpson KM, Aggarwal N, Clancy Jr J, Jilka RL: Effect of the mi allele on mast cells, basophils, natural killer cells, and osteoclasts in C57Bl/6J mice. J Cell Physiol 1987, 132:565–570
4. Stevens J, Loutit JF: Mast cells in spotted mutant mice (W Ph mi). Proc R Soc Lond B Biol Sci 1982, 215:405–409
5. Chabot B, Stephenson DA, Chapman VM, Besmer P, Bernstein A: The proto-oncogene c-kit encoding a transmembrane tyrosine kinase receptor maps to the mouse W locus. Nature 1988, 335:88–89
6. Geissler EN, Ryan MA, Housman DE: The dominant-white spotting (W) locus of the mouse encodes the c-kit proto-oncogene. Cell 1988, 55:185–192
7. Huang E, Nocka K, Beier DR, Chu TY, Buck J, Lahm HW, Wellner D, Leder P, Besmer P: The hematopoietic growth factor KL is encoded by the Sl locus and is the ligand of the c-kit receptor, the gene product of the W locus. Cell 1990, 63:225–233
8. Zsebo KM, Williams DA, Geissler EN, Broudy VC, Martin FH, Atkins HL, Hsu RY, Birkett NC, Okino KH, Murdock DC, Jacobsen FW, Langley KE, Smith KA, Takeishi T, Cattanach BM, Galli SJ, Suggs SV: Stem cell factor is encoded at the Sl locus of the mouse and is the ligand for the c-kit tyrosine kinase receptor. Cell 1990, 63:213–224
9. Flanagan JG, Leder P: The kit ligand: a cell surface molecule altered in steel mutant fibroblasts. Cell 1990, 63:185–194
10. Williams DE, Eisenman J, Baird A, Rauch C, Van Ness K, March CJ, Park LS, Martin U, Mochizuki DY, Boswell HS, Burgess GS, Cosman D, Lyman SD: Identification of a ligand for the c-kit proto-oncogene. Cell 1990, 63:167–174
11. Hodgkinson CA, Moore KJ, Nakayama A, Steingrimsson E, Copeland NG, Jenkins NA, Arnheiter H: Mutations at the mouse microphthalmia locus are associated with defects in a gene encoding a novel basic-helix-loop-helix-zipper protein. Cell 1993, 74:395–404
12. Morii E, Ogihara H, Kim DK, Ito A, Oboki K, Lee YM, Jippo T, Nomura S, Maeyama K, Lamoreux ML, Kitamura Y: Importance of leucine zipper domain of mi transcription factor (MITF) for differentiation of mast cells demonstrated using mi(ce)/mi(ce) mutant mice of which MITF lacks the zipper domain. Blood 2001, 97:2038–2044
13. Morii E, Ogihara H, Oboki K, Kataoka TR, Maeyama K, Fisher DE, Lamoreux ML, Kitamura Y: Effect of a large deletion of the basic domain of mi transcription factor on differentiation of mast cells. Blood 2001, 98:2577–2579
14. Kitamura Y, Morii E, Jippo T, Ito A: Mi-transcription factor as a regulator of mast cell differentiation. Int J Hematol 2000, 71:197–202

15. Kitamura Y, Morii E, Jippo T, Ito A: Effect of MITF on mast cell differentiation. Mol Immunol 2002, 38:1173–1176
16. Kitamura Y, Morii E, Jippo T, Ito A: Regulation of mast cell phenotype by MITF. Int Arch Allergy Immunol 2002, 127:106–109
17. Enerback L: Berberine sulphate binding to mast cell polyanions: a cytofluorometric method for the quantitation of heparin. Histochemistry 1974, 42:301–313
18. Jippo T, Morii E, Ito A, Kitamura Y: Effect of anatomical distribution of mast cells on their defense function against bacterial infections: demonstration using partially mast cell-deficient tg/tg mice. J Exp Med 2003, 197:1417–1425
19. Galli SJ, Kitamura Y: Genetically mast-cell-deficient W/Wv and Sl/Sld mice. Their value for the analysis of the roles of mast cells in biologic responses in vivo. Am J Pathol 1987, 127:191–198
20. Wershil BK, Mekori YA, Murakami T, Galli SJ: 125I-fibrin deposition in IgE-dependent immediate hypersensitivity reactions in mouse skin. Demonstration of the role of mast cells using genetically mast cell-deficient mice locally reconstituted with cultured mast cells. J Immunol 1987, 139:2605–2614
21. Wershil BK, Murakami T, Galli SJ: Mast cell-dependent amplification of an immunologically nonspecific inflammatory response. Mast cells are required for the full expression of cutaneous acute inflammation induced by phorbol 12-myristate 13-acetate. J Immunol 1988, 140: 2356–2360
22. Matsuda H, Kawakita K, Kiso Y, Nakano T, Kitamura Y: Substance P induces granulocyte infiltration through degranulation of mast cells. J Immunol 1989, 142:927–931
23. Yano H, Wershil BK, Arizono N, Galli SJ: Substance P-induced augmentation of cutaneous vascular permeability and granulocyte infiltration in mice is mast cell dependent. J Clin Invest 1989, 84:1276–1286
24. Lawman MJ, Boyle MD, Gee AP, Young M: A rapid technique for measuring leukocyte chemotaxis in vivo. J Immunol Methods 1984, 69:197–206
25. Nakahata T, Spicer SS, Cantey JR, Ogawa M: Clonal assay of mouse mast cell colonies in methylcellulose culture. Blood 1982, 60:352–361
26. Kitamura Y, Kawata T, Suda O, Ezumi K: Changed differentiation pattern of parental colony-forming cells in F1 hybrid mice suffering from graft-versus-host disease. Transplantation 1970, 10:455–462
27. Bernstein SE: Acute radiosensitivity in mice of differing W genotype. Science 1962, 137:428–429
28. Morii E, Oboki K, Jippo T, Kitamura Y: Additive effect of mouse genetic background and mutation of MITF gene on decrease of skin mast cells. Blood 2003, 101:1344–1350
29. Iwamoto I, Tomoe S, Tomioka H, Yoshida S: Leukotriene B4 mediates substance P-induced granulocyte infiltration into mouse skin. Comparison with antigen-induced granulocyte infiltration. J Immunol 1993, 151:2116–2123
30. Mencia-Huerta JM, Razin E, Ringel EW, Corey EJ, Hoover D, Austen KF, Lewis RA: Immunologic and ionophore-induced generation of leukotriene B4 from mouse bone marrow-derived mast cells. J Immunol 1983, 130:1885–1890
31. Levi-Schaffer F, Dayton ET, Austen KF, Hein A, Caulfield JP, Gravallese PM, Liu FT, Stevens RL: Mouse bone marrow-derived mast cells cocultured with fibroblasts. Morphology and stimulation-induced release of histamine, leukotriene B4, leukotriene C4, and prostaglandin D2. J Immunol 1987, 139:3431–3441
32. Kitamura Y, Shimada M, Go S: Presence of mast cell precursors in fetal liver of mice. Dev Biol 1979, 70:510–514
33. Ito A, Koma Y, Watabe K, Jippo T, Wakayama T, Iseki S, Kitamura Y: Contribution of the Sg IGSF adhesion molecule to survival of cultured mast cells in vivo. Biochem Biophys Res Commun 2004, 319:200–206
34. Peters EM, Maurer M, Botchkarev VA, Jensen K, Welker P, Scott GA, Paus R: Kit is expressed by epithelial cells in vivo. J Invest Dermatol 2003, 121:976–984
35. Matsuda H, Kitamura Y, Sonoda T, Imori T: Precursor of mast cells fixed in the skin of mice. J Cell Physiol 1981, 108:409–415
36. Morii E, Oboki K, Ishihara K, Jippo T, Hirano T, Kitamura Y: Roles of MITF for development of mast cells in mice: effects on both precursors and tissue environments. Blood (in press)
37. Echtenacher B, Mannel DN, Hultner L: Critical protective role of mast cells in a model of acute septic peritonitis. Nature 1996, 381:75–77
38. Malaviya R, Ikeda T, Ross E, Abraham SN: Mast cell modulation of neutrophil influx and bacterial clearance at sites of infection through TNF-alpha. Nature 1996, 381:77–80